Characterizing venom resistance in *Monodelphis domestica* yields new insights into mammalian blood physiology

Matthew Holding*[2,3], Dante Disharoon*[4], Laura Haynes*[2], Bipin Chakravarthy Paruchuri[4], M. Hao Hao Pontius[7], Krista Golden[7], Jordan A. Shavit[7,8], Karl Desch[7], David Ginsburg[2,7,8,9], Anirban Sen Gupta[4], Yolanda Cruz[6], Danielle H. Drabeck[1]

*Joint first authors
Corresponding author: Danielle H. Drabeck

[1]Department of Ecology, Evolution, and Behavior, University of Minnesota, Twin Cities
[2]Life Sciences Institute, University of Michigan, Ann Arbor, MI
[3]Department of Ecology and Evolutionary Biology, University of Michigan, Ann Arbor, MI, USA
[4]Department of Biomedical Engineering, Case Western Reserve University, Cleveland, OH 44106, USA.
[6]Oberlin College Department of Biology, Oberlin, OH 44074, USA
[7]Department of Pediatrics, University of Michigan, Ann Arbor, MI, USA
[8]Departments of Human Genetics, University of Michigan, Ann Arbor, MI, USA
[9]Departments of Internal Medicine, University of Michigan, Ann Arbor, MI, USA

Interactions between predators and prey are often characterized by strong selection that shapes extreme physiological adaptations for survival in hostile environments. Venom resistance in large-bodied South American opossums (Clade Didelphini) provides a striking example as they are well known to prey upon snakes and have strong resistance to extremely toxic snake venom. While resistance is well known in this group of large-bodied opossums, relatively little is known about the venom resistance of the remaining diverse and speciose members of Didelphidae (small-bodied opossums) that inhabit the same regions in South America and encounter the same venomous snakes. Here, we investigate the venom resistance of *Monodelphis domestica* through multi-level physiological assays, examining responses to both purified venom components and whole venom from sympatric and allopatric vipers. Our results reveal that *M. domestica* exhibits significant resistance to venom-induced blood coagulation, retains normal platelet function in the presence of venoms that are known to disrupt platelet function, and has enhanced inhibition of snake venom metalloproteinases. Unexpectedly, we find a previously unknown modification of opossum blood physiology, namely, that opossum von Willebrand Factor (VWF) requires increased shear force to elongate, which may contribute to the venom resistance phenotype and has relevance to human coagulopathic disease. Together these data expand the known extent of venom resistance beyond the large-bodied clade, suggesting it is a widespread adaptive trait in South American marsupials. This work provides new insights into venom-mammal coevolution by expanding our understanding of the physiological adaptations underlying venom resistance including how they can inspire biomedical solutions to coagulation disorders.

Introduction

Interactions between venomous species and their enemies offer striking examples of coevolution, where molecular adaptations on both sides drive dynamic physiological changes. Mammalian venom resistance represents an extreme outcome of coevolution, where molecular changes enable mammals to withstand the injection of deadly toxins from venomous species. Such systems offer a powerful model for understanding how molecular changes—like those in proteins targeted by venom— are shaped by strong selective pressure, impose costs on physiological function, and facilitate adaptive ecologies.

South American large-bodied opossums in the clade Didelphini are well-known to be resistant to venomous pit-vipers with which they are sympatric (Jansa and Voss 2011; Drabeck et al. 2020, 2022). Large-bodied opossums in this clade regularly prey upon venomous snakes, and resistance to venom is thought to be primarily a trophic adaptation which allows them to exploit an otherwise lethal prey resource (Voss and Jansa 2012). Venom resistance in the large-bodied opossums has been relatively well characterized, and is known to be especially effective against snakes in the genus *Bothrops*, which are the most abundant and widely distributed venomous snakes across South America (Werner and Vick 1977; Voss and Jansa 2012; Holding et al. 2016b; Engelman et al. 2017; Drabeck et al. 2020; Voss and Jansa 2021; Drabeck et al. 2022).

Small-bodied South American opossums are both abundant and speciose across the same range of venomous snakes and have long been assumed to be venom-susceptible prey (Mackessy 2021), rather than predators, of venomous snakes (notable exception (Voss 2013)). Consequently, the role of small-bodied opossums in the ecology and evolution of venom (and resistance to venom), has been previously assumed to be inconsequential. However, recent research has identified resistance to botrocetin, a venom C-type lectin (CTL) from *Bothrops jararaca*, in a small-bodied species (*Monodelphis domestica)* suggesting that this species may enjoy venom resistance similar to its large-bodied relatives in Didelphini (Drabeck et al. 2020).

In venom-susceptible mammals, botrocetin induces coagulopathy by binding to von Willebrand Factor (VWF), triggering VWF to interact with the platelet receptor GP1bα (Fukuda et al. 2002). VWF is a multimeric protein that circulates in plasma in a globular conformation. During vascular injury, VWF becomes exposed to elevated shear stresses which causes it to unravel, exposing its A domains (Lenting et al. 2024). In the absence of venom proteins, VWF plays a vital physiologic role with platelets to prevent unwanted bleeding via two crucial mechanisms: 1) its A3 domain binds to subendothelial collagen (exposed by vessel injury), anchoring it to the injury site, and 2) its A1 domain binds to platelet GP1bα receptor, rendering rapid platelet accumulation (Lenting et al. 2024). Upon binding to VWF, platelets become activated and these aggregate with each other via fibrinogen binding through integrin GPIIb/IIIa, resulting in the formation of a platelet plug. Venom-derived VWF-binding CTLs cause damage by binding to the A1 domain of VWF and promoting complexation with platelets even in low shear conditions (Matsushita et al. 2000; Fukuda et al. 2002). The resulting CTL-VWF-platelet complex

gets rapidly cleared from circulation, thereby depleting VWF and platelets from circulation, rendering them unavailable for hemostatic platelet plug formation (extreme thrombocytopenia), causing excessive bleeding and death (Matsushita et al. 2000; Fukuda et al. 2002; Bury et al. 2019; Thomazini et al. 2021). This disruption in platelet function is thought to work synergistically with hemorrhagic metalloproteinases in *Bothrops* venom, which degrade vascular tissues by cleaving proteins in the basal lamina, causing widespread bleeding and tissue damage.

Comparative analyses have identified mutations in VWF coding sequences across several small-bodied opossum species, including *Monodelphis domestica*, that are predicted to disrupt botrocetin binding and confer resistance (Drabeck et al. 2022). Protein binding assays confirmed that VWF from both small and large-bodied opossums binds poorly to multiple VWF-targeting CTLs, such as botrocetin, aspercetin, and bitiscetin, suggesting that mutations on VWF disrupt binding of venom CTLs and potentially facilitate resistance (Drabeck et al. 2022). These disruptive mutations on VWF have independently evolved multiple times across both large and small-bodied opossums, indicating strong selective pressure on VWF regions associated with venom CTL resistance (Drabeck et al. 2022). However, though previous studies demonstrated that *Monodelphis domestica* platelets do not respond to botrocetin as human platelets do, and that an *E.coli* expressed opossum VWF A1 domain fails to bind to venom CTLs, understanding of venom resistance in this species remains extremely limited. Firstly*, in vitro* aggregation assays used previously provide only a coarse measure of total venom-induced platelet response in a cuvette (not in a living organism), leaving subsequent physiological responses, such as platelet adhesion or fibrin formation, which contribute to the organism's overall resistance, unexplored. These assays may also lead to an over-estimation of venom resistance, as it is possible that though *M. domestica* VWF fails to bind to botrocetin, it may still suffer poor platelet adhesion and delayed fibrin formation similar to venom susceptible species (essentially voiding the impact of mutations on VWF on its ability to resist CTLs). The degree of impact of venom CTLs on these downstream physiologies is required to understand the true impact of venom CTLs on this species, and more generally the robustness of previous works' assertion that *M. domestica* enjoys venom resistance comparable to its large-bodied cousins (Drabeck et al. 2020, 2022).

Secondly, the behavior of blood and all its component parts can be greatly altered by experiments that are conducted outside of a blood vessel. For example, shear force (the force per unit area acting on the vessel wall caused by blood flow through the vessel) plays a crucial role in the physiological function of VWF, as it promotes the unfolding of VWF multimers, enabling platelet adhesion and clot formation at sites of vascular injury. For example, VWF-CTL binding might be promoted under flow conditions, making *M. domestica* less resistant than predicted by previous *in vitro* protein-protein interactions measured in absence of flow. Evaluating the response of VWF to venom CTLs under vascularly relevant flow conditions is therefore essential to understanding the extent to which venom resistant species might maintain normal function in the presence of venom proteins. Lastly, resistance to individual venom components, such as VWF-targeting CTLs, does not necessarily translate to whole-venom resistance across all physiological systems. CTLs represent only one class within the

diverse suite of venom proteins (e.g. metalloproteinases and phospholipases), for which resistance in this species is completely unexamined.

Understanding the mechanistic basis of an extreme adaptation like venom resistance requires a systems-level approach, integrating multiple physiological processes to capture the full scope of how these animals survive repeated venom exposures. The current study aimed to characterize venom resistance in *M. domestica* across multiple physiological scales, and for multiple types of venoms. We predicted that *M. domestica* would exhibit specific resistance to *Bothrops jararaca* venom, with minimal disruption of platelet function and superior inhibition of venom metalloproteinases relative to humans and other mammals. Our data confirm that *M. domestica* has significant multifaceted venom resistance that is species-specific and aligns with known ecological interactions. Our data unexpectedly reveal that *M. domestica* requires a higher shear rate to initiate elongation compared to human VWF, an unpredicted but potentially consequential aspect of opossum physiology which may also contribute to venom resistance. This research provides insight into the complex mechanistic basis of venom resistance in small-bodied opossums and provides vital physiological insights, which may guide novel therapeutic strategies for VWF-related bleeding disorders.

Methods

Venom and Protein Purification

Purified fractions of botrocetin from *Bothrops jararaca* and aspercetin from *Bothrops asper,* bitiscetin from *Bitis arietans*, as well as whole venom from *Bothrops jararaca* were used from previous work (Drabeck et al. 2020, 2022)(botrocetin B). Convulxin was purchased from ChemCruz (Santa Cruz Biotechnology Inc, Santa Cruz, CA). Whole venom from *Crotalus oreganus* and *Sistrurus miliarius* was obtained during previous studies (Gibbs et al. 2011). Venom CTLs were chosen to best provide a direct comparison of physiological and protein assays done in previous work (Drabeck et al. 2020, 2022).

Opossum Handling and Blood Collection

Opossums (n= 16) were housed in the Oberlin research colony and cared for according to procedures previously described (Rousmaniere et al. 2010). To collect blood for VWF purification, opossums (*Monodelphis domestica*) were sacrificed by first being placed under isoflurane sedation and then exsanguinated via the posterior vena cava, per IACUC protocol F23BBYC-1 (Keyte and Smith 2008). Samples used for VWF purification were collected in an ACD-coated syringe (acid citrate dextrose Solution A) and preserved in vacutainers containing the same solution (BD Pharmaceuticals). Samples used in all other assays were collected in 3.2% sodium citrate coated syringe and similarly placed in vacutainers containing the same solution (BD pharmaceuticals). Human blood was collected from de-identified donors via venipuncture into 3.2% sodium citrate vacutainers (BD Pharmaceuticals) by the Case Western Reserve University Hematopoietic Biorepository and Cellular Therapy Core under an Institutional Review Board (IRB)-approved protocol (Case 12Z05, IRB # 09-90-195) of University Hospitals Cleveland Medical Center. Blood was then centrifuged at 150 rcf for 15 min at 25°C to isolate a

platelet-rich plasma (PRP) supernatant, which was removed without disturbing the buffy coat. The remaining sample was then centrifuged at 2000 rcf for 25 minutes to recover platelet-poor plasma which was later used for dilutions and standards.

Venom Inhibition Assays

We evaluated the inhibition of whole venom by *Monodelphis domestica* serum against three snake venoms (*Bothrops jararaca*, *Crotalus oreganus*, and *Bitis arietans*) using a modified protocol from the EnzChek Gelatinase/Collagenase Assay Kit (Life Technologies, Carlsbad, CA, USA). Briefly, this assay tests the ability of *Monodelphis domestica* serum to neutralize venom-induced degradation of a gelatin substrate, which mimics the extracellular matrix proteins targeted by snake venom metalloproteinases (SVMPs), and other enzymatic venom components (Holding et al. 2016a). The DQ-gelatin substrate was diluted to 1:20 in reaction buffer for the assay.

Serum was taken from opossums during venous blood extraction and frozen for subsequent analyses, and the protein concentration of each serum sample determined with the Pierce BCA Protein Assay Kit. Venom samples were diluted to a final protein concentration of 0.3125 ng per well. Venom was incubated with various amounts of *M. domestica* serum, with 0, 5, 10, 25, 50, 125, 250, or 475 µg serum protein per well, to determine the extent of venom inhibition.

Fluorescence intensity was measured in relative fluorescence units (RFU) using a SpectraMax M2 microplate reader (Molecular Devices) at 30 second intervals. The slope of the fluorescence increase (RFU min^{-1}) from the linear portion of the reaction curve was calculated to quantify the venom's SVMP (snake venom metalloproteinase) activity. Decreased slope values, as compared to control reactions with no serum, indicate successful inhibition of venom enzymatic activity by the serum. Each experiment was performed in triplicate, and data were normalized to the control (untreated venom) to calculate relative SVMP activity.

Dose-dependence curves were fitted using the drc package in R, with a four-parameter logistic model for each serum treatment (opossum, squirrel, and human) (Ritz et al. 2015). Human plasma was used as a non-coevolved venom-sensitive baseline for venom SVMP inhibition by serum proteins, and squirrel (*Otospermophilus beecheyi*) was used to compare species-specific inhibition as it has previously been shown to have resistance for its sympatric predator (*Crotalus oreganus*) (Holding et al. 2016a). Venoms were selected to represent 1) a sympatric species (*Bothrops jararaca*) for which ecological and other data predict resistance, 2) an allopatric species (*Crotalus oreganus*) for which another mammal (ground squirrels) have evolved venom resistance 3) an allopatric distantly related viper (*Bitis arietans*) (Figure 2 top and middle panels).

Aggregation Assays

To test *M. domestica*'s ability to resist whole venom as well as isolated CTLs, whole blood aggregation was assessed using an impedance aggregometer (Roche multiplate aggregometer). Briefly, these assays differ from microfluidic assays as coagulopathic response is indicated by *induction* of platelet aggregation, rather than inhibition. In the absence of

212 exposed collagen and/or shear force, platelets in blood (in a stationary cuvette) should not
213 rapidly aggregate unless exposed to a platelet activating agonist (i.e. whole venom or pure
214 venom-derived CTLs). Failure of agonists to induce platelet aggregation suggests strong venom
215 resistance to coagulopathic venom components, including CTLs. Thus, we expect *M.*
216 *domestica*'s platelet aggregation response to be lower for sympatric venom and CTLs than for
217 allopatric venom and CTLs, suggesting higher resistance to species they have evolved with.
218 Platelet aggregation response in this assay is measured by impedance, where higher
219 impedance means a greater response. Purified CTLs used were aspercetin (20 µL, 0.1 mg/mL),
220 convulxin (20 µg, 0.01 mg/mL), and botrocetin (20 µg, 0.01 mg/mL). Platelet aggregation was
221 measured over 10 minutes, with impedance changes recorded as a measure of platelet
222 aggregation. All purified CTLs were selected from South American vipers that were either
223 completely sympatric (*Bothrops jararaca*), partially sympatric (*Crotalus durissus*), or allopatric
224 (*Bothrops asper*) with *M. domestica*. It should be noted that while aspercetin and botrocetin
225 induce aggregation via VWF, convulxin induces aggregation via a direct interaction with the
226 platelet. In addition to purified CTLs, we also challenged *M. domestica* with whole venom from
227 the same sympatric species (*Bothrops jararaca*), as well as two distantly related allopatric
228 species with vastly diverse venoms (*Crotalus adamanteus* and *Sistrurus miliarius*) to provide
229 some measure of the specificity/cross-reactivity of venom resistance in *M. domestica* in the
230 absence of availability of whole venom from *Bothrops asper* and *Crotalus durissus* (see Figure 3
231 range maps).
232 Venous blood samples collected from *M. domestica* in 3.2% sodium citrate tubes were
233 tested within four hours of collection at room temperature. For each assay, 300 µl citrated
234 whole blood and 300 µl NaCl/CaCl2 solution (0.9% saline and 3mM CaCl2 provided my
235 manufacturer) were aliquoted into cuvettes and stirred at 37°C. Aggregation was induced by
236 adding 20 µL of agonists to the samples. Collagen (20 µg/mL) was used as a positive control,
237 PBS (phosphate buffered saline) was used as a negative control, Aggregation response was
238 calculated as the average of two replicate measures. To facilitate cross-comparison, the data
239 were normalized by subtracting the minimum value within each treatment group, ensuring that
240 the minimum impedance value was zero. Data visualization was performed using R software to
241 allow for comparison of platelet responses to different agonists. Venom assay and controls
242 were conducted in triplicate to ensure reproducibility; however, due to limited plasma volume,
243 CTL tests were not replicated.
244
245 *VWF Multimer Gel*
246 Opossum VWF was purified by size-exclusion chromatography at 4ºC as previously
247 described (De Marco and Shapiro 1981), using plasma pooled after high-speed centrifugation.
248 Fractions were quantitated by absorbance at 280 nm using the in-line detector on the AKTA
249 Pure. To ascertain that VWF from *M. domestica* bound to microchannel equine-derived type 1
250 fibrillar collagen (Chrono-log Corporation), purified and quantified opossum VWF was tagged
251 with Alexa488 using the Alexa Fluor 488 (AF488) Microscale Protein Labelling Kit (Invitrogen)
252 with minor modification for subsequent microchannel runs. The remaining untagged VWF was
253 frozen and stored at -80C.

254 To compare opossums' VWF multimer structure to human, we performed a multimer
255 analysis using VWF purified from *M. domestica* plasma and HumateP (a purified human
256 plasma-derived product that contains VWF and Factor VIII, CSL Behring). Due to the enormous
257 size of intact VWF multimers, agarose is used instead of polyacrylamide. VWF multimers were
258 analyzed by electrophoresis using a 1.6% separating LDS agarose gel and visualized using the
259 rabbit anti-human VWF antibody A0082 (DAKO) as previously described (Pruss et al. 2011).
260 Protein was transferred to nitrocellulose using the semi-dry Power Blotter (ThermoFisher) and
261 western blot was performed using the iBind Flex (Invitrogen) system with the rabbit anti-human
262 VWF antibody A0082 (DAKO) as primary and IRDye 800CW anti-rabbit antibody (Li-Cor). Lanes
263 were visualized a Li-Cor Odyssey CLx Imager and Image Studio (LiCor).
264
265 *Microfluidic Assays*
266 To evaluate whether the apparent resistance of *M. domestica* to CTL-induced platelet
267 aggregation (Figure 3) could be protective against bleeding, we performed microfluidics assays
268 developed to approximate *in vivo* injury conditions which allowed for real-time measurement of
269 VWF/VWFplatelet recruitment and fibrin generation.
270 Microfluidics experiments were performed in the Bioflux 200 system (Cell
271 Microsystems) using 48-well High Shear Plates (Cell Microsystems) (Conant et al. 2009; Girish
272 et al. 2022). Glass-bottomed microfluidic channels with a width of 250 µm and a height of 70
273 µm were coated with 100 µg/mL type 1 equine fibrillar collagen (Chrono-log Corporation) in 20
274 µM acetic acid for 60 min at 37°C. These conditions facilitate the self-polymerization of
275 collagen fibers which anchor to the glass substrate, creating an environment which mimics
276 collagen exposure following vascular injury. Unbound collagen was washed by perfusing 0.1
277 wt% bovine serum albumin (BSA) in calcium-free phosphate buffered saline (PBS) at 30
278 dyn/cm^2 for 2 min.
279 While we have previously standardized this assay for use with human blood, it was
280 unknown whether the equine collagen would allow binding of opossum VWF in a similar manner
281 and under similar shear flow conditions. To verify that this assay is applicable to opossum VWF,
282 we used purified and fluorescently tagged VWF to determine experimental conditions and verify
283 that opossum VWF binds effectively to equine fibrillar collagen used in standard microfluidics
284 assays (Figure 1). AF488-labeled human or opossum VWF in calcium-free PBS was perfused
285 through the collagen-coated microfluidic channel at shear stresses ranging from 20 to 200
286 dyn/cm^2. VWF binding to collagen was imaged under epifluorescence using a Zeiss Axio
287 Observer microscope with a 10x objective (Plan-NEOFLUAR, NA = 0.3). We observed similar
288 overall VWF deposition, indicating that opossum VWF binds to equine collagen to a similar
289 extent as human VWF. We further observed that opossum VWF required comparatively higher
290 shear flow conditions (80 dyn/cm^2 for opossum VWF vs. 60 dyn/cm^2 for human VWF) to fully
291 elongate, which we discuss in detail in the results and elsewhere (Figure 1).
292 With assay conditions established, we assessed the ability of *M. domestica* to resist the
293 detrimental effects of venom CTLs. Opossum or human (as a venom non-resistant control
294 species) blood was processed and used to perform assays within four hours of any given draw,
295 to ensure that platelet activity in the blood remained viable. Citrated PRP was obtained as

296 described in the *Opossum Handling and Blood Collection* section. PRP was incubated with 1
297 µg/mL calcein-AM (Invitrogen) to stain platelets and 10 µg/mL AF-647 fibrinogen (Invitrogen)
298 for 30 min at room temperature. Samples were recalcified to 20 mM $CaCl_2$ and immediately
299 perfused through collagen-coated channels at 60 dyn/cm^2, a shear condition that is relevant to
300 wound environments. These conditions provide more fine-tuned information about the degree
301 and type of physiological response induced by exposed collagen in the presence of agonists.
302 Epifluorescence microscopy was used to image platelet accumulation and fibrin generation in
303 real time. Samples were run without any additives (Control) to assess normal platelet adhesion
304 and fibrin generation. For each sample, complementary assays were performed in the presence
305 of three venom derived CTLs known to affect platelet aggregation function: botrocetin,
306 aspercetin, and convulxin. Each CTL was used at its ED_{90} concentration for human blood: 4
307 µg/mL for botrocetin, 20 µg/mL for aspercetin, and 0.5 µg/mL for convulxin. In this assay, we
308 expect that CTL-induced VWF/platelet complexation leading to thrombocytopenia and low VWF
309 levels should result in reduced platelet adhesion and prolonged fibrin generation times,
310 mimicking bleeding observed *in vivo*. To account for differences in platelet counts between
311 individual animals, platelet adhesion was normalized to the control condition for each sample.
312
313
314
315
316
317 **Results**
318
319 *Venom Inhibition*
320 While hemostatic disruptions are an important mechanism of venom pathology,
321 enzymatic tissue damage caused by venom proteinases often make up the majority of viper
322 venoms and are thought to be a major source of venom pathology. To address the ability of M.
323 domestica's serum to inhibit this functional component of venom, we employed gelatin-based
324 inhibitions assays. Gelatinase inhibition assays test the ability of blood serum from different
325 species to inhibit the ability of venom to break down a substrate that mimics tissue and are
326 typically used as a proxy quantitation of venom metalloproteinase (SVMP) inhibition. These
327 data are used to calculate ED_{90} values, which represent the dosage of serum needed to inhibit
328 90% of the venom's gelatinase activity. Blood serum from *M. domestica* demonstrated varying
329 levels of inhibition across the three snake venoms tested: *Bothrops jararaca*, *Crotalus oreganus*,
330 and *Bitis arietans* (Figure 2A-C; Table 1). In all cases, increasing concentrations of serum protein
331 led to a dose-dependent decrease in venom proteinase activity. For *Bothrops jararaca* venom
332 (Figure 2A), *M. domestica* serum rapidly inhibited SVMP activity at the middle to high
333 concentrations of serum protein tested, resulting in the lowest ED_{90} value of the three sera
334 tested, indicating it inhibited venom approximately 2.5 times better than squirrel serum and 14
335 times better than human serum (Table 1). Similarly, serum of the squirrel *O. beecheyi* yielded a
336 lower ED_{90} for its sympatric predator, *C. oreganus*, than did the human or opossum sera (Table

1). Finally, opossum serum performed best against the venom of the African viper *B. arietans,* while human and squirrel serum showed overlapping trends in inhibition.

Whole Blood Aggregation

Whole blood aggregation assays revealed differential platelet responses by *M. domestica* to the various venoms and purified CTLs tested (Figure 3). As shown in Figure 3A, collagen, used as a positive control, induced a rapid and sustained increase in impedance, indicative of expected collagen-induced platelet aggregation, while PBS (negative control) established a baseline throughout the 10-minute measurement period.

Among whole venoms, *Crotalus adamanteus* venom elicited the most pronounced platelet aggregation response, with impedance peaking around 5 minutes at approximately 220% of the collagen control (400 Ω) before showing pronounced disaggregation, indicating a robust but transient aggregation effect (Figure 3). *Sistrurus miliarius* venom induced a response reaching approximately 70% of the collagen control (180 Ω), while *Bothrops jararaca* venom resulted in a minimal increase in impedance, remaining just slightly below the PBS baseline (50 Ω), suggesting substantial resistance to platelet activation (Figure 3). As expected, collagen (positive control) produced a peak impedance of 180 Ω, while PBS (baseline control) showed negligible effects with impedance remaining below 50 Ω, which is consistent with standard values for other mammals (Baumgarten et al. 2010; Nash et al. 2017).

The purified CTLs demonstrated variable effects on platelet aggregation. Convulxin, a known collagen-like agonist, induced a notable increase in impedance, mirroring the aggregation pattern of the collagen control but with a delayed onset (Figure 3). Consistent with whole venom results which showed no resistance to *Crotalus* venom, this indicates a lack of resistance to Convulxin (derived from *Crotalus durissus* venom). Aspercetin, which targets VWF, triggered a measurable but extremely reduced platelet aggregation response. Botrocetin, like whole *B. jararaca* venom, elicited no detectable platelet aggregation response. The responses of both aspercetin and botrocetin observed here are extremely minimal compared to previously well-established responses for susceptible species, suggesting strong resistance (Rucavado et al. 2001: Figure 4; Drabeck et al. 2020: Figure 3). Overall, *M. domestica* showed the lowest levels of whole blood aggregation by both snake venom and purified CTLs from their sympatric snake predators in the genus *Bothrops* and appeared to be entirely resistant to both platelet disturbance by *B. jararaca* venom and botrocetin. This is consistent with the hypothesis of evolution of increased resistance to venom of sympatric snakes in *M. domestica*.

VWF Multimers

In humans, higher molecular weight VWF multimers are more procoagulant than lower weight forms as they are more likely to bind platelets after interacting with subendothelial collagen under flow. When compared to a commercial preparation of human VWF, no obvious differences in multimer distribution between *Monodelphis domestica* and human VWF were observed. Both displayed a typical distribution of high, intermediate, and low molecular weight multimers (Supplementary Figure 1) although it is easier to visualize the higher molecular weight multimers in *M. domestica* due to the higher concentration of this sample. This suggests

379 that the multimerization process is preserved in *M. domestica* and indicates that this VWF is
380 structurally comparable to human VWF in terms of multimer formation, despite sequence
381 divergence associated with phylogenetic distance or selective changes in VWF function.
382
383 *Platelet Adhesion and Fibrin Generation in Microfluidics*
384 Blood clot formation relies on rapid platelet adhesion at sites of vascular injury,
385 followed by aggregation and fibrin clot formation to stabilize the plug. While aggregation assays
386 measure platelet clumping under static conditions, they do not replicate *in vivo* conditions
387 because aggregometry assays do not have endothelium and vasculature or shear forces (i.e.
388 vascular-relevant flow). Microfluidic assays better recapitulate these physiological conditions
389 by simulating blood flow along vessel walls using pressurized synthetic vessels with
390 immobilized collagen attached to the 'vessel' wall, providing insights into how venom
391 components modulate platelet function and disrupt hemostasis. Consequently, microfluidic
392 assays can recapitulate the *in vivo* effects of venom components, that is, *inhibition* of platelet
393 plug formation (platelet adhesion and aggregation) at sites of vascular injury and the
394 subsequent development of fibrin clots.
395 As expected, control experiments with human PRP showed that platelet accumulation
396 on the microfluidic surface was strongly inhibited by botrocetin and convulxin, and weakly
397 inhibited by aspercetin (Figure 4A-D).Venom derived CTLs also significantly reduced platelet
398 fluorescence in *Monodelphis domestica* PRP (Figure 4 E-H); however, the defect was less
399 pronounced after treatment with botrocetin or convulxin than in human PRP (Figure 4 B, F, D, H),
400 suggesting some measure of resistance to those CTLs. In human PRP, the initial rate of platelet
401 adhesion was similar for the control, botrocetin and aspercetin conditions, but reduced to
402 almost zero in the presence of convulxin (as indicated by the initial slope of the platelet
403 fluorescence curves, Figure 4I). A similar trend was observed in opossum PRP, except that
404 platelets adhered even in the presence of convulxin, though at much lower levels than the other
405 conditions (Figure 4J). Concordant with the whole blood aggregometry analyses, the effect of
406 botrocetin on platelet adherence to the microchannel was decreased in *M. domestica* (Figure 4
407 B, F, J): botrocetin caused a more severe defect in the total extent of platelet adhesion than
408 aspercetin in human PRP, but a less severe defect than aspercetin in opossum PRP (Figure 4I-
409 K). Aspercetin and convulxin caused a similar response in both species (Figure 4K). Concordant
410 with the whole blood aggregometry analyses, the effect of botrocetin on platelet adherence to
411 the microchannel was significantly decreased in *M. domestica* when compared to human
412 (Figure 4 B & F, K). In human PRP, botrocetin caused a 66 ± 16% reduction in the overall extent
413 of platelet adhesion compared to the negative control, whereas it only caused a 39 ± 15%
414 reduction in opossum PRP (Figure 4K).
415 We further quantified the fibrin generation kinetics (by quantifying 'lag time' reflecting
416 the time needed for fibrin clot formation), where a prolonged lag time is unfavorable for
417 effective hemostasis and predictive of bleeding. Purified venom CTLs increased lag time in both
418 humans and opossums (Figure 4 L-N). While convulxin had a dramatic effect in human samples,
419 abrogating fibrin formation almost completely, it showed a more modest response in opossums
420 (Figure 4 L-N). As with platelet adhesion, the greatest signal for resistance was seen in

421 botrocetin treatments (Figure 4 L-N), with an overall reduced effect of botrocetin in opossum
422 PRP (Figure 4 L-N). Botrocetin caused a nearly threefold increase in fibrin lag time from 3.6 ±
423 1.0 min to 9.0 ± 1.2 min in human PRP, but a statistically insignificant prolongation of fibrin lag
424 time in opossum PRP (from 3.1 ± 0.8 to 4.5 ± 1.8 min, Figure 4N).
425 Surprisingly, aspercetin caused a statistically insignificant prolongation in the fibrin lag
426 time for human PRP but doubled lag time from 3.1 ± 0.8 min to 7.4 ± 2.4 min in opossum PRP,
427 which is perhaps suggestive of opossum susceptibility to aspercetin. This result is consistent
428 with previously established weak affinity of aspercetin to VWF A1 in protein binding assays and,
429 together with weak platelet adhesion inhibition observed here, suggests that VWF-mediated
430 platelet aggregation is not the primary function of coagulopathy for aspercetin (Drabeck et al.
431 2022).
432 Convulxin induced a reduced coagulopathy in opossum PRP compared to human PRP
433 but remained the most potent effector of integrated hemostatic function in both species.
434 Platelet fluorescence and adhesion in response to aspercetin was roughly similar between
435 human and opossum, though aspercetin had a slightly stronger effect on fibrin lag time in
436 opossums. Compared to humans, *M. domestica* VWF showed a measurably reduced integrated
437 coagulopathic response (platelet fluorescence, platelet adhesion, and fibrin lag time) to
438 botrocetin, suggesting that these opossums have functionally meaningful hemostatic protective
439 effects against this CTL.
440
441
442 **Discussion**
443 Understanding the physiological mechanisms, molecular underpinnings, and
444 evolutionary history of venom resistance across opossums is crucial for understanding how
445 selective pressures, ecological interactions, and physiological constraints shape the evolution
446 of such extreme adaptations (Byrne et al. 2014; Xu et al. 2020). Our results provide compelling
447 evidence that *M. domestica* possesses considerable resistance to both CTLs and whole venom
448 from *Bothrops jararaca*, and suggests that previous *in vitro* work showing convergently derived
449 mutations on VWF is indicative of venom resistance (Drabeck et al. 2022). We also uncover a
450 previously undescribed modification to opossum VWF, that it requires a greater shear force to
451 elongate, potentially contributing to the resistance phenotype or other important adaptive
452 physiologies.
453 Under normal conditions, VWF will be induced to elongate and bind platelets in response
454 to either exposed collagen (mimicking vessel damage) or under increased shear force (caused
455 by increased blood flow after vessel damage), creating a primary platelet plug preceding the
456 formation of a more stable cross-linked fibrin clot (Sadler 1998; Ruggeri 2003). Botrocetin is
457 known to induce coagulopathy upon introduction to the body by binding to VWF (at the A1
458 domain) and inducing VWF to elongate and attach to platelets (Matsushita et al. 2000; Fukuda
459 et al. 2002). Botrocetin then changes conformation slightly and binds secondarily to the platelet
460 GP1Bα binding site, creating a tight trimolecular complex which renders platelets unavailable for
461 adhesion and causes extreme thrombocytopenia (Fukuda et al. 2002, 2005). More recently,
462 detailed physiological work on botrocetin has shown that in the presence of VWF, botrocetin

can induce coagulopathy even in the absence of its preferred platelet receptor (GP1Bα), and that it also interacts directly with a different platelet integrin (αIIbβ3) to block fibrinogen and other ligands essential for coagulation and healing (Shen et al. 2024). While aspercetin is also a VWF-mediated agonist from a closely related viper (*Bothrops asper*) and is thought to work in a similar manner because of its ability to induce VWF-mediated platelet agglutination, detailed structural studies have yet to locate its exact binding site on VWF and prior kinetics studies show weak binding to the A1 domain (Rucavado et al. 2001; Drabeck et al. 2022). Integrated coagulopathic data shown in this work supports that VWF-mediated platelet activity is a weak action for aspercetin and may not be the main mode of coagulopathy for this CTL. Convulxin is derived from the more distantly related tropical rattlesnake *Crotalus durissus*, and binds directly to the GPVI platelet receptor, inducing coagulopathy independent of VWF (Batuwangala et al. 2004).

Our assays of whole blood aggregation revealed a reduced response of *M. domestica* blood to both botrocetin and aspercetin but not convulxin. Initially, this might lead us to assume that opossum resistance is specific to CTLs from *Bothrops spp.* and centered at VWF. However, microfluidic assays showed that platelet adhesion and fibrin clot formation in opossums was more disrupted by aspercetin than botrocetin. This suggests that the molecular changes that have previously been found to abolish binding between opossum VWF and botrocetin result in resistance to this CTL (implying specificity), but *does not* result in resistance to aspercetin, despite the appearance of strong resistance that would be gleaned from aggregation data alone. Aspercetin appears to be able to function nearly as well in opossums as it does in humans in microfluidics assays (in both cases it has weak function), but not in whole blood assays, highlighting the importance of integrated assays which capture a more complete picture of coagulopathic function. These results suggest that aspercetin may act directly on platelets, fibrin, or other agonists more strongly during platelet adhesion and fibrin clot formation, or that its function in opossum depends on the presence of shear force. Given that its action in humans is also weak relative to other CTLs, and previous work has revealed a surprisingly low affinity for human VWF compared to other VWF-mediated agonists, it is possible that this is an accessory function of this protein, or that its affinity for VWF is specific to a non-mammalian VWF target.

Similarly, we observed a tremendously decreased coagulopathic response in opossums (compared to previously established human responses) to whole venoms from both species of *Bothrops*, but not *Crotalus*. Opossum serum showed superior ability to inhibit the enzymatic action of whole venom for all species tested, except *Crotalus oreganus*, which was best inhibited by its sympatric prey (*Otospermophilus beecheyi*). Interestingly, *M. domestica* serum very strongly inhibited venom from the African viper, *Bitis arietans*, which points to the likelihood that this species also possesses generalized inhibitory proteins (snake venom metalloproteinase inhibitors, phospholipase inhibitors), similar to those seen in other highly resistant taxa (Voss and Jansa 2012).

Bothrops spp. are well known to interact with opossums and are a known prey item of several species of South American opossums (Voss and Jansa 2012; Voss 2013). *Bothrops jararaca* co-occurs across the range of *M. domestica*, are relatively small and gracile, semi-

arboreal, and have been anecdotally observed to bite *M. domestica* without effect (Martins et al. 2001; Da Silva et al. 2024; exclusivo cuíca predando cascavel e coral verdadeira e é picado por elas n.d.). *Bothrops asper* are somewhat closely related to *B. jararaca;* however they are much larger and their range does not overlap with *M. domestica*. Previous work examining diet in small-bodied opossums has suggested that predator-prey relationships between opossums and snakes may role-switch relative to factors affecting venom potency like geographic region, body size, and age (Voss 2013). Conversely, *Crotalus durissus* is documented to be prey of only the larger bodied opossums (Didelphini) and though its range overlaps with *M. domestica*, our data did not reveal compelling evidence that *M. domestica* has profound resistance to convulxin (the CTL derived from its venom) (Almeida-Santos et al. 2000; Voss and Jansa 2012). This suggests that small-bodied opossum venom resistance may be more specialized for species that they target for prey, are appropriately sized for prey, or that are more abundant in their environment.

Interestingly, our findings reveal that VWF in *M. domestica* requires a comparatively higher shear force than that for human VWF, to elongate. This property could have important implications for venom resistance by making it more difficult for venom components, like botrocetin, to bind VWF and exact subsequent coagulopathic effects. Elevated shear thresholds for VWF elongation may also protect against other physiological disruptions, such as spontaneous platelet adhesion in high-flow conditions or inappropriate clot formation. Beyond venom resistance, this trait may be linked to broader physiologies of non-placental mammals, potentially reflecting differences in vascular dynamics, metabolism, or reproductive strategies. The discovery of this and potentially other species with shear-resistant VWF may also provide a novel avenue for therapeutic exploration, where engineering similar shear-resistant VWF variants could help prevent bleeding disorders associated with left ventricular assist devices (LVAD) (Nascimbene et al. 2016). While there is some limited data to suggest that increased shear elongation may occur in other venom resistant species (pigs), little is known about the diversity of this trait across species, or what potential costs and tradeoffs it might evoke (Chan et al. 2017). Further work is merited to better understand this unique physiology and explore its potential for inspiring new strategies for mitigating LVAD-related complications and other vascular disorders.

Our work adds detailed multi-layered comparative assays using physiologic vessel models to already mounting evidence that venom resistance is present in small-bodied marsupials, and demonstrates the ability of comparative phylogenetic work to inform otherwise cryptic adaptations and ecologies (Jansa and Voss 2011; Drabeck et al. 2020, 2022). In light of these findings, it is likely that many more of the opossum species identified to have similar and convergently evolved changes in VWF may have similar degrees of venom resistance (Drabeck et al. 2022). Further work is warranted to examine the true ecological roles and behaviors of this entire group of mammals and emphasizes a need for basic natural history work. This work also provides vital insight into the evolution of venom in this region and suggests that South American viper venoms may have evolved in the presence of many more species of co-evolving venom-resistant mammalian predators and prey than previously assumed. Detailed physiological data presented here serves to further inform the physiological mechanisms,

relative strength, and specificity of this extreme adaptation, and provides key insights for future work aiming to understand the molecular basis and evolution of this remarkable trait.

Acknowledgements

The authors would like to thank Alexandra Rucavado, Erika Hingst-Zaher, and the Kentucky Reptile Zoo for their help in acquisition and purification of venoms used for this work. Authors on this work were supported by the Minnesota IRACDA Program 2K12GM119955 (NIGMS, NIH), the NSF STEM-APWD (DEB 2316784), NIH R01-HL121212, NIH R35-HL171421, and NIH R35-HL150784 (NHLBI). The authors would like to thank Suzanne McGaugh for tremendous guidance as well as lab and resource support. The authors would also like to thank Marvin Neiman (Case Western), Alison Narayan/Sarah Ackenhusen (University of Michigan), and Randy Westrick (Oakland University) for their guidance, feedback, and support.

Tables

Table 1. Species-specific ED_{90} values (µg/mL) derived from dose-response analysis of SVMP inhibition by increasing amounts of serum protein from three mammal species. ED_{90} (Effective Dose, 90%) indicates the amount of serum required to inhibit 90% of the venom's proteinase activity. Asterisks indicate species that are sympatric with the snake venom tested.

Source of Venom	Serum	ED_{90}	S.E.
Bothrops jararaca	Human	12379.2	6272.4
	Opossum*	865.4	149.1
	Squirrel	2182.2	636.7
Crotalus oreganus	Human	11391.6	7660.1
	Opossum	1236.6	231.7
	Squirrel*	541.9	71.4
Bitis arietans	Human	774.4	80.1
	Opossum	220.5	21.7
	Squirrel	940.5	107.7

Figure Legends

Figure 1. (A) Elongation of von Willebrand Factor (VWF) under different shear conditions. (B)The degree of elongation for both human and *Monodelphis domestica* (opossum) VWF under varying shear forces in

a microfluidics assay. Purified VWF was fluorescently tagged and perfused across collagen-coated channels at shear rates of 0 dyn/cm² to 200 dyn/cm² for human and opossum samples, respectively. The percentage elongation of VWF was quantified and normalized to both the 0 dyn/cm^2 condition (0% elongation) and the 200 dyn/cm^2 condition (100% elongation). At 60 dyn/cm², human VWF showed full elongation, whereas opossum VWF remained partially coiled, indicating that higher shear rates are required to induce full elongation in the latter. When perfused at 80 dyn/cm², opossum VWF fully elongated, mirroring the response observed in human VWF at 60 dyn/cm^2. Error bars represent the average ± SD of n = 10 replicates. High degrees of fluorescent labeling caused aggregation or "clumping" of VWF multimers in both human and possum samples, inhibiting complete elongation. Reduced labeling allowed full elongation for human VWF at 60 dyn/cm², but opossum VWF still required the higher shear rate (80 dyn/cm²) to achieve comparable uncoiling.

Figure 2. Range maps for mammals *M. domestica* and *O. Beechyi* (top), and snakes (B. jararaca, *C. oreganus*, and *B. arietans* (middle). Bottom panel shows results of the venom inhibition assays. *Bothrops jararaca*, *Crotalus oreganus*, and *Bitis arietans* venoms were incubated with increasing concentrations of mammalian serum (*M. domestica*, *O. Beechyi*, and *H. sapiens*), and relative degradation of a gelatin substrate was measured. Data points represent the mean ± SEM for three independent experiments. *M. domestica* serum demonstrated greater inhibition of proteinase activity compared to squirrel and human sera, at higher serum concentrations, particularly for venoms from *B. jararaca* and *B. arietans*. Inhibition was assessed based on the reduction in fluorescence due to the degradation of a gelatin substrate, reflecting the venom's proteolytic activity. In this graph, the x axis would represent total resistance (depicted with the alive mouse icon), and decrease as you move away from y = 0 (depicted by the dead mouse icon).

Figure 3. Platelet aggregation *in Monodelphis domestica* whole blood in response to venoms and purified C-type lectins. Impedance was measured over a 10-minute period to assess platelet aggregation response. (A) Collagen (positive control), and PBS (negative control). (B) Whole venoms (*Crotalus adamanteus*, *Sistrurus miliarius*, and *Bothrops jararaca*) are in the middle panels. (C) C-type lectins, Convulxin (derived from *Crotalus durissus* venom), aspercetin (derived from *Botrhops asper* venom) and botrocetin (derived from *Bothrops jararaca* venom) are on the bottom panels. Data represents the average impedance change over time, normalized to account for baseline variation. Multiple curves represent independent samples (replicates) performed when available. Cartoon on the left depicts platelet aggregation (lowest at y =0 and increases at higher values of y). Range maps of species from which each venom/CTL are derived are shown in the upper right of each graph to allow for a comparison of aggregation response with sympatry.

Figure 4. Compared to humans, opossums exhibited resistance to botrocetin (bot), but not aspercetin (asp) or convulxin (cvx). A-H) Endpoint images of platelet (fluorescently labeled in green) adhesion to a collagen coated substrate after 10 min of shear flow at 60 dyn/cm^2. A) Human platelet rich plasma (h-PFP) perfused across a collagen-coated substrate resulted in robust platelet adhesion in the absence of venom derivatives (ctrl). B) Platelet adhesion was significantly reduced in the presence of bot, C) moderately reduced in the presence of asp, D) and almost completely abrogated in the presence of cvx. E) Compared to h-PRP, opossum PRP (o-PRP) exhibited a similar extent of platelet adhesion to collagen. F) However, platelet adhesion was affected to a lesser extent by bot. H) o-PRP responded similar to h-PRP to asp, but H) platelet adhesion in o-PRP was not entirely abolished by cvx. I-J) Representative quantification of platelet fluorescence over time. I) In h-PRP, the overall extent of platelet adhesion was

622 reduced slightly by asp, significantly by bot, and almost completely by cvx. J) Though platelet adhesion in
623 o-PRP was affected by asp to a similar degree as h-PRP, platelet adhesion was only barely reduced by
624 bot. Some degree of platelet adhesion was preserved in the presence of cvx. K) Aggregate platelet
625 adhesion data, normalized to the ctrl condition for each individual donor or opossum. The defect in
626 platelet adhesion was similar for h-PRP and o-PRP for asp and cvx, but reduced significantly in o-PRP for
627 bot. L-M) Representative quantification of fibrin(ogen) fluorescence over time. The sharp ramp indicates
628 fibrin generation, and the corresponding time point is parameterized as fibrin lag time. L) In h-PRP, fibrin
629 polymerized quickly in the absence of venom derivatives, owing to the procoagulant surface of collagen-
630 bound platelets. Asp and bot both delayed the formation of fibrin, with bot having a more pronounced
631 effect. Fibrin did not polymerize during the 10 min experiment in the presence of cvx. M) In o-PRP, bot
632 caused only a marginal prolongation in fibrin lag time. Both asp and cvx significantly delayed fibrin
633 generation. N) Aggregate fibrin generation data. The dashed line at t = 10 min indicates the endpoint of
634 the experiment. On average, fibrin generated in less than 4 min in h-PRP. Bot more than doubled fibrin lag
635 time, with half of the replicates not generating fibrin within the 10 min experimental window. Despite its
636 similarity to bot, asp did not significantly affect fibrin lag time. In three of four replicates, fibrin did not
637 generate within 10 min in the presence of cvx. In o-PRP, fibrin lag time was prolonged by asp and cvx, but
638 not bot. o-PRP generated fibrin faster than h-PRP in the presence of bot or cvx, but slower than h-PRP in
639 the presence of asp. Statistics were performed using one-way ANOVA using Fisher's LSD correction. Error
640 bars mean ± SD. For significance, *: $p \leq 0.05$, **: $p \leq 0.01$, *** $p \leq 0.001$, ****$p \leq 0.0001$.
641
642
643
644 **Supplementary Figure 1.** Opossum VWF Multimer Gel 1.6% resolving + 0.8% stacking Tris Glycine LDS-
645 SeaKem HGT Agarose Vertical Multimer Gel (8x8cm vertical). Multimeric structures of von Willebrand
646 factor (VWF) were analyzed using a 1.6% lithium dodecyl sulfate (LDS) agarose gel under non-reducing
647 conditions. Lane 2 contained 30 µL of purified Monodelphis domestica VWF (heated at 60°C for 30
648 minutes) and 10µl loading buffer. Lane 5 contained 30 µL HumateP (human VWF) as a control (heated at
649 60°C for 30 minutes) and 10µl loading buffer. The gel was transferred to a nitrocellulose membrane and
650 visualized by fluorescence with anti-human VWF antibody (Dako A0082) using a Li-Cor Odyssey CLx
651 Imaging System (Li-Cor).
652
653

654 ## References

655

656 Almeida-Santos, S. M., M. M. Antoniazzi, O. A. Sant'Anna, and C. Jared. 2000. Predation by the Opossunn
657 Didelphis marsupialis on the Rattlesnake Crotalus durissus. Curr.Herpetol. 19:1–9.

658 Batuwangala, T., M. Leduc, J. M. Gibbins, C. Bon, and E. Y. Jones. 2004. Structure of the snake-venom
659 toxin convulxin. Acta Crystallogr D Biol Crystallogr 60:46–53.

660 Baumgarten, A., M. Wilhelmi, K. Kalbantner, M. Ganter, and R. Mischke. 2010. Measurement of platelet
661 aggregation in ovine blood using a new impedance aggregometer. Veterinary Clinical Pathology
662 39:149–156.

663 Bury, L., A. Malara, S. Momi, E. Petito, A. Balduini, and P. Gresele. 2019. Mechanisms of thrombocytopenia
664 in platelet-type von Willebrand disease. Haematologica 104:1473–1481.
665 Byrne, R. T., A. J. Klingele, E. L. Cabot, W. S. Schackwitz, J. A. Martin, J. Martin, Z. Wang, E. A. Wood, C.
666 Pennacchio, L. A. Pennacchio, N. T. Perna, J. R. Battista, and M. M. Cox. 2014. Evolution of
667 extreme resistance to ionizing radiation via genetic adaptation of DNA repair. eLife 3:e01322.
668 eLife Sciences Publications, Ltd.
669 Chan, C. H. H., I. L. Pieper, C. R. Robinson, Y. Friedmann, V. Kanamarlapudi, and C. A. Thornton. 2017.
670 Shear Stress-Induced Total Blood Trauma in Multiple Species. Artificial Organs 41:934–947.
671 Conant, C. G., M. A. Schwartz, T. Nevill, and C. Ionescu-Zanetti. 2009. Platelet adhesion and aggregation
672 under flow using microfluidic flow cells. J Vis Exp 1644.
673 Da Silva, F. F. B., T. D. A. Moura, T. Siqueira-Silva, J. M. Gutiérrez, and P. A. Martinez. 2024. Predicting the
674 drivers of Bothrops snakebite incidence across Brazil: A Spatial Analysis. Toxicon 250:108107.
675 Drabeck, D. H., A. Rucavado, E. Hingst-Zaher, Y. P. Cruz, A. M. Dean, and S. A. Jansa. 2020. Resistance of
676 South American opossums to vWF-binding venom C-type lectins. Toxicon 178:92–99.
677 Drabeck, D. H., A. Rucavado, E. Hingst-Zaher, A. Dean, and S. A. Jansa. 2022. Ancestrally Reconstructed
678 von Willebrand Factor Reveals Evidence for Trench Warfare Coevolution between Opossums and
679 Pit Vipers. Molecular Biology and Evolution 39:msac140.
680 Engelman, R. K., F. Anaya, and D. A. Croft. 2017. New palaeothentid marsupials (Paucituberculata) from
681 the middle Miocene of Quebrada Honda, Bolivia, and their implications for the palaeoecology,
682 decline and extinction of the Palaeothentoidea. Journal of Systematic Palaeontology 15:787–
683 820.
684 Fukuda, K., T. A. Doggett, L. A. Bankston, M. A. Cruz, T. G. Diacovo, and R. C. Liddington. 2002. Structural
685 Basis of von Willebrand Factor Activation by the Snake Toxin Botrocetin. Structure 10:943–950.
686 Fukuda, K., T. Doggett, I. J. Laurenzi, R. C. Liddington, and T. G. Diacovo. 2005. The snake venom protein
687 botrocetin acts as a biological brace to promote dysfunctional platelet aggregation. Nat Struct
688 Mol Biol 12:152–159.

689 Gibbs, H. L., L. Sanz, J. E. Chiucchi, T. M. Farrell, and J. J. Calvete. 2011. Proteomic analysis of
690 ontogenetic and diet-related changes in venom composition of juvenile and adult Dusky Pigmy
691 rattlesnakes (*Sistrurus miliarius barbouri*). Journal of Proteomics 74:2169–2179.
692 Girish, A., K. Jolly, N. Alsaadi, M. de la Fuente, A. Recchione, R. An, D. Disharoon, Z. Secunda, S.
693 Raghunathan, N. F. Luc, C. Desai, E. Knauss, X. Han, K. Hu, H. Wang, U. D. S. Sekhon, N. Rohner, U.
694 A. Gurkan, M. Nieman, M. D. Neal, and A. Sen Gupta. 2022. Platelet-Inspired Intravenous
695 Nanomedicine for Injury-Targeted Direct Delivery of Thrombin to Augment Hemostasis in
696 Coagulopathies. ACS Nano 16:16292–16313.
697 Holding, M. L., J. E. Biardi, and H. L. Gibbs. 2016a. Coevolution of venom function and venom resistance
698 in a rattlesnake predator and its squirrel prey. Proceedings of the Royal Society B: Biological
699 Sciences 283:20152841. Royal Society.
700 Holding, M. L., D. H. Drabeck, S. A. Jansa, and H. L. Gibbs. 2016b. Venom Resistance as a Model for
701 Understanding the Molecular Basis of Complex Coevolutionary Adaptations. Integrative and
702 Comparative Biology 56:1032–1043.
703 Jansa, S. A., and R. S. Voss. 2011. Adaptive Evolution of the Venom-Targeted vWF Protein in Opossums
704 that Eat Pitvipers. PLOS ONE 6:e20997. Public Library of Science.
705 Keyte, A. L., and K. K. Smith. 2008. Harvesting *Monodelphis* Embryos. Cold Spring Harb Protoc
706 2008:pdb.prot5074.
707 Lenting, P. J., C. V. Denis, and O. D. Christophe. 2024. How unique structural adaptations support and
708 coordinate the complex function of von Willebrand factor. Blood 144:2174–2184.
709 Mackessy, S. P. 2021. Handbook of Venoms and Toxins of Reptiles. CRC Press.
710 Martins, M., M. S. Araujo, R. J. Sawaya, and R. Nunes. 2001. Diversity and evolution of macrohabitat use,
711 body size and morphology in a monophyletic group of Neotropical pitvipers (*Bothrops*). Journal
712 of Zoology 254:529–538.
713 Matsushita, T., D. Meyer, and J. E. Sadler. 2000. Localization of von Willebrand Factor-binding Sites for
714 Platelet Glycoprotein Ib and Botrocetin by Charged-to-Alanine Scanning Mutagenesis. Journal of
715 Biological Chemistry 275:11044–11049.

716 Nascimbene, A., S. Neelamegham, O. H. Frazier, J. L. Moake, and J. Dong. 2016. Acquired von Willebrand
717 syndrome associated with left ventricular assist device. Blood 127:3133.
718 Nash, K. J., L. M. Bacek, P. W. Christopherson, and E. A. Spangler. 2017. In vitro effect of blood cell counts
719 on multiple-electrode impedance aggregometry in dogs. , doi: 10.2460/ajvr.78.12.1380.
720 Pruss, C. M., M. Golder, A. Bryant, C. A. Hegadorn, E. Burnett, K. Laverty, K. Sponagle, A. Dhala, C. Notley,
721 S. Haberichter, and D. Lillicrap. 2011. Pathologic mechanisms of type 1 VWD mutations R1205H
722 and Y1584C through in vitro and in vivo mouse models. Blood 117:4358–4366.
723 Ritz, C., F. Baty, J. C. Streibig, and D. Gerhard. 2015. Dose-Response Analysis Using R. PLOS ONE
724 10:e0146021. Public Library of Science.
725 Rousmaniere, H., R. Silverman, R. A. White, M. M. Sasaki, S. D. Wilson, J. T. Morrison, and Y. P. Cruz. 2010.
726 Husbandry of Monodelphis domestica in the study of mammalian embryogenesis. Lab Anim
727 39:219–226.
728 Rucavado, A., M. Soto, A. Kamiguti, D. Theakston, J. Fox, T. Escalante, and J. M. Gutiérrez. 2001.
729 Characterization of Aspercetin, a Platelet Aggregating Component from the Venom of the Snake
730 Bothrops asper which Induces Thrombocytopenia and Potentiates Metalloproteinase-induced
731 Hemorrhage. Thromb Haemost 85:710–715.
732 Ruggeri, Z. M. 2003. Von Willebrand factor, platelets and endothelial cell interactions. Journal of
733 Thrombosis and Haemostasis 1:1335–1342.
734 Sadler, J. E. 1998. BIOCHEMISTRY AND GENETICS OF VON WILLEBRAND FACTOR. Annu. Rev. Biochem.
735 67:395–424.
736 Shen, C., D. T. Mackeigan, A. A. Shoara, P. Bhoria, G. Zhu, D. Karakas, W. Ma, Z. Y. Chen, R. Xu, S.
737 Slavkovic, D. Zhang, V. Prifti, Z. Liu, E. G. Cerenzia, P. Chen, M. A. D. Neves, H. Li, F. Xue, R. Yang,
738 J. Liu, R. Lai, R. Li, and H. Ni. 2024. Novel GPIb-independent platelet aggregation induced by
739 botrocetin: implications for diagnosis and antithrombotic therapy. Journal of Thrombosis and
740 Haemostasis S1538783624004471.
741 Thomazini, C. M., A. T. A. Sachetto, C. Z. De Albuquerque, V. G. De Moura Mattaraia, A. K. De Oliveira, S.
742 M. D. T. Serrano, I. Lebrun, K. C. Barbaro, and M. L. Santoro. 2021. Involvement of von Willebrand

743 factor and botrocetin in the thrombocytopenia induced by Bothrops jararaca snake venom. PLoS
744 Negl Trop Dis 15:e0009715.
745 Voss, R. S. 2013. Opossums (Mammalia: Didelphidae) in the diets of Neotropical pitvipers (Serpentes:
746 Crotalinae): Evidence for alternative coevolutionary outcomes? Toxicon 66:1–6.
747 Voss, R. S., and S. A. Jansa. 2021. Opossums: An Adaptive Radiation of New World Marsupials. JHU
748 Press.
749 Voss, R. S., and S. A. Jansa. 2012. Snake-venom resistance as a mammalian trophic adaptation: lessons
750 from didelphid marsupials. Biological Reviews 87:822–837.
751 Werner, R. M., and J. A. Vick. 1977. Resistance of the opossum (Didelphis virginiana) to envenomation by
752 snakes of the family Crotalidae. Toxicon 15:29–32.
753 Xu, S., J. Wang, Z. Guo, Z. He, and S. Shi. 2020. Genomic Convergence in the Adaptation to Extreme
754 Environments. Plant Comm 1. Elsevier.
755 N.d. exclusivo cuíca predando cascavel e coral verdadeira e é picado por elas.
756

Mammal Range Maps

Monodelphis domestica

Otospermophilus beecheyi

Snake Range Maps

Bothrops jararaca

Crotalus oreganus

Bitis arietans

Venom Inhibition Assays

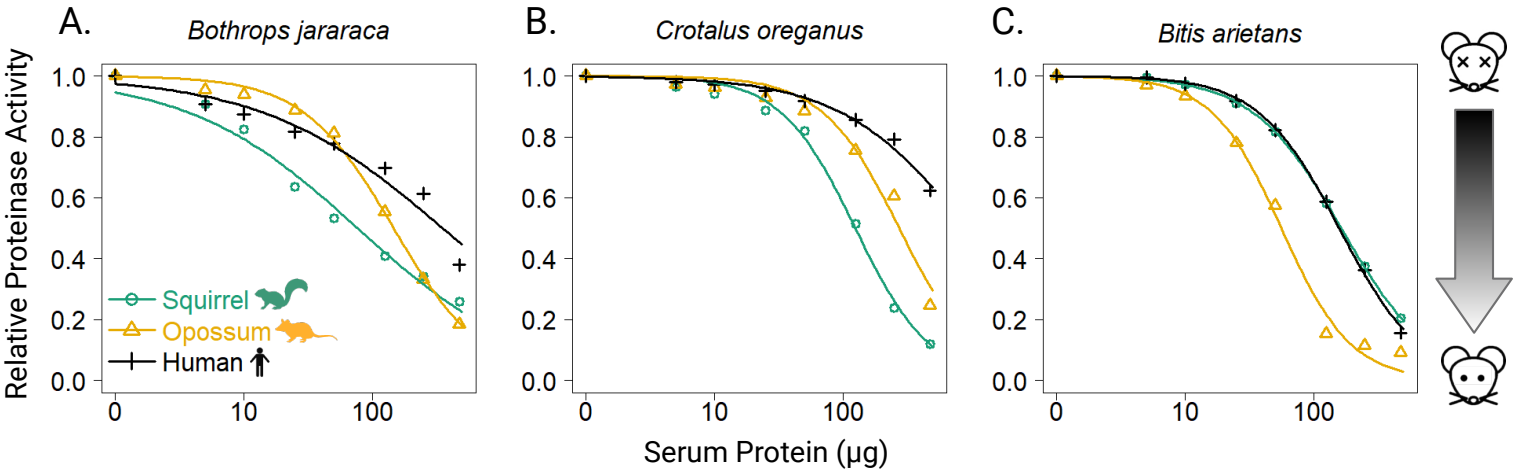

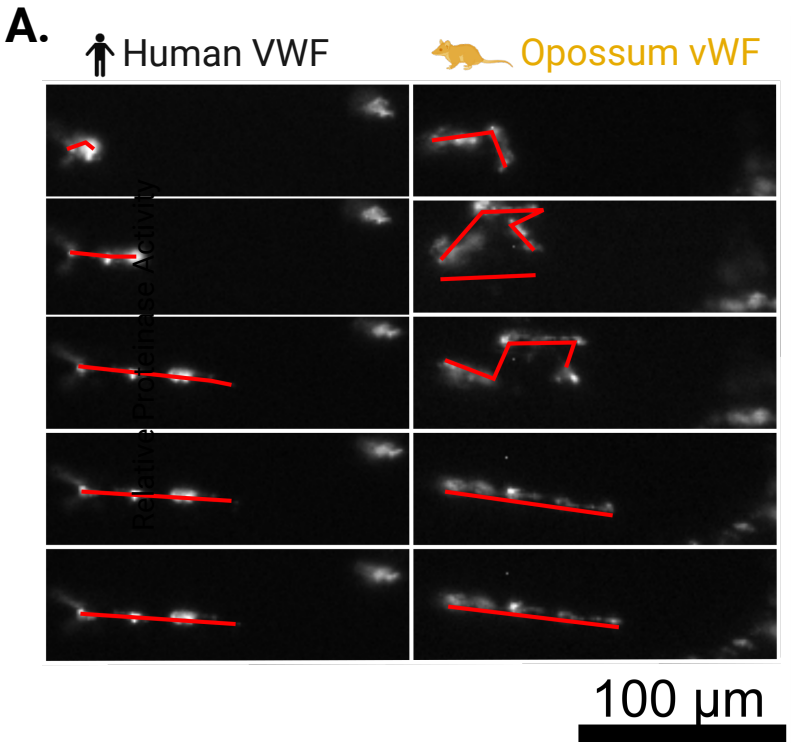
A.
Human VWF
Opossum vWF
100 µm

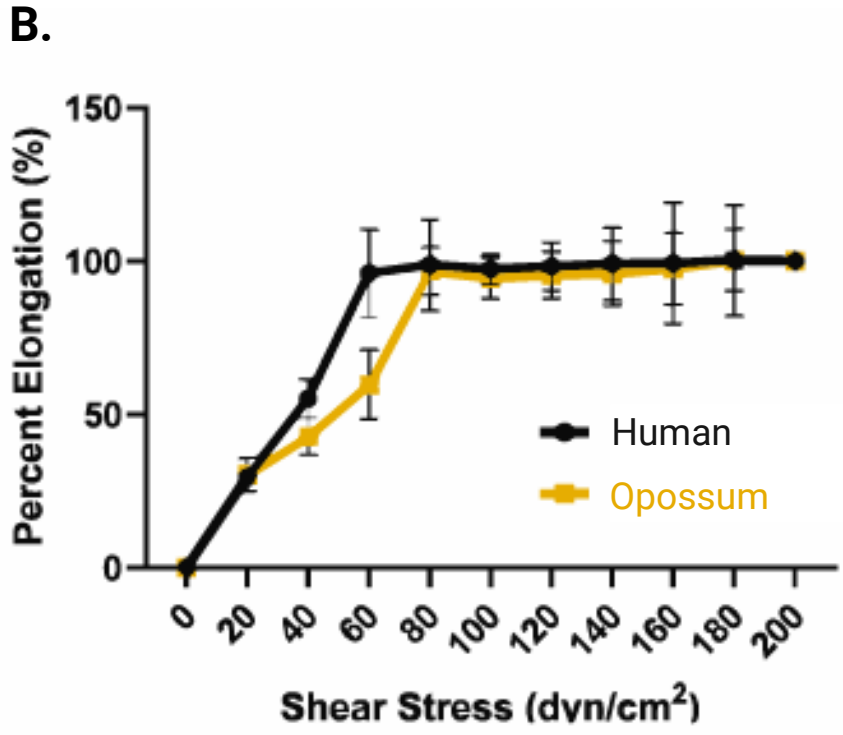
B.
Percent Elongation (%)
150
100
50
0
0
20
40
60
80
100
120
140
160
180
200
Shear Stress (dyn/cm²)
Human
Opossum

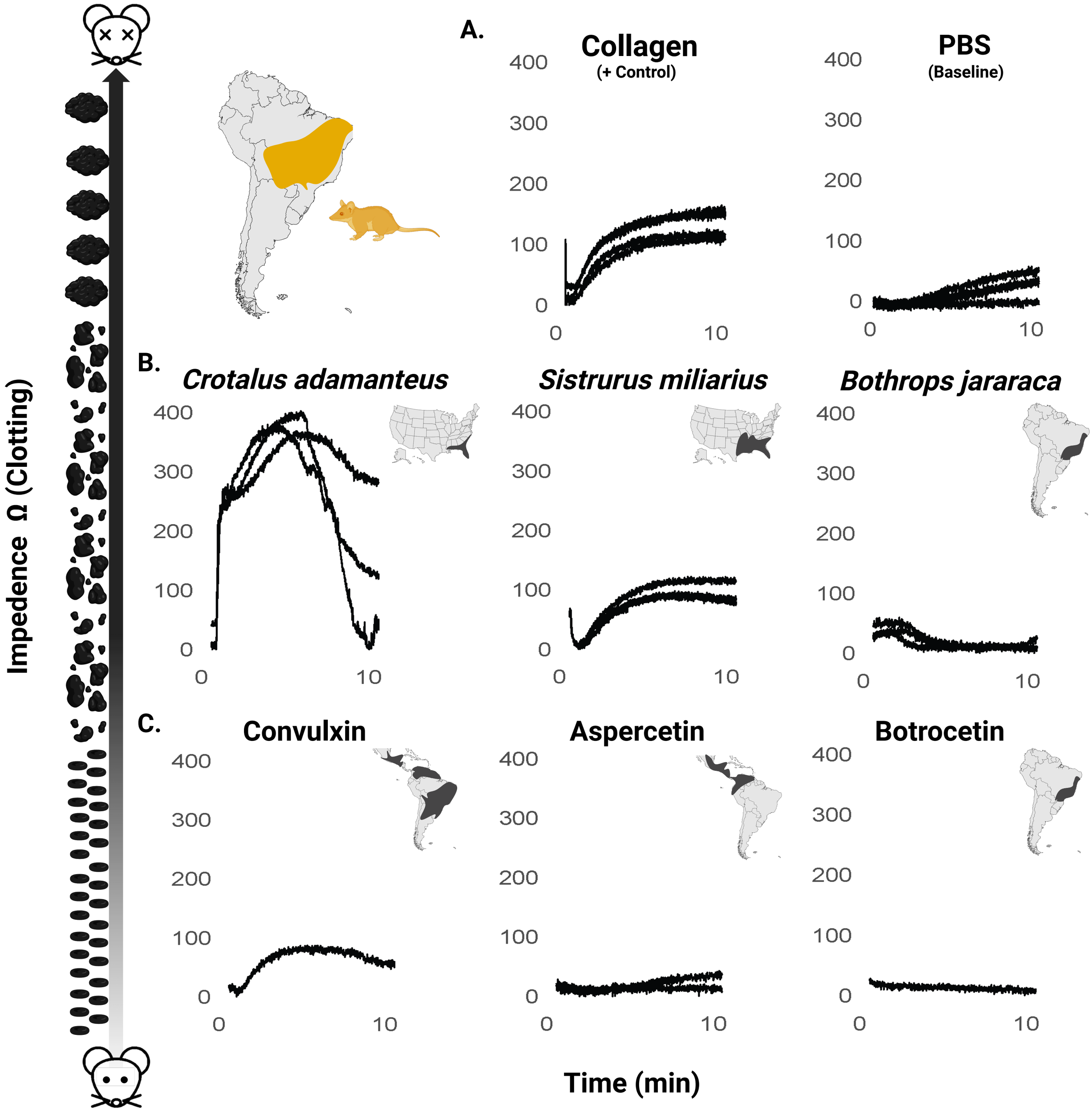
A.
Collagen
(+ Control)
PBS
(Baseline)
B.
Crotalus adamanteus
Sistrurus miliarius
Bothrops jararaca
C.
Convulxin
Aspercetin
Botrocetin
Impedence Ω (Clotting)
Time (min)
0
100
200
300
400
10

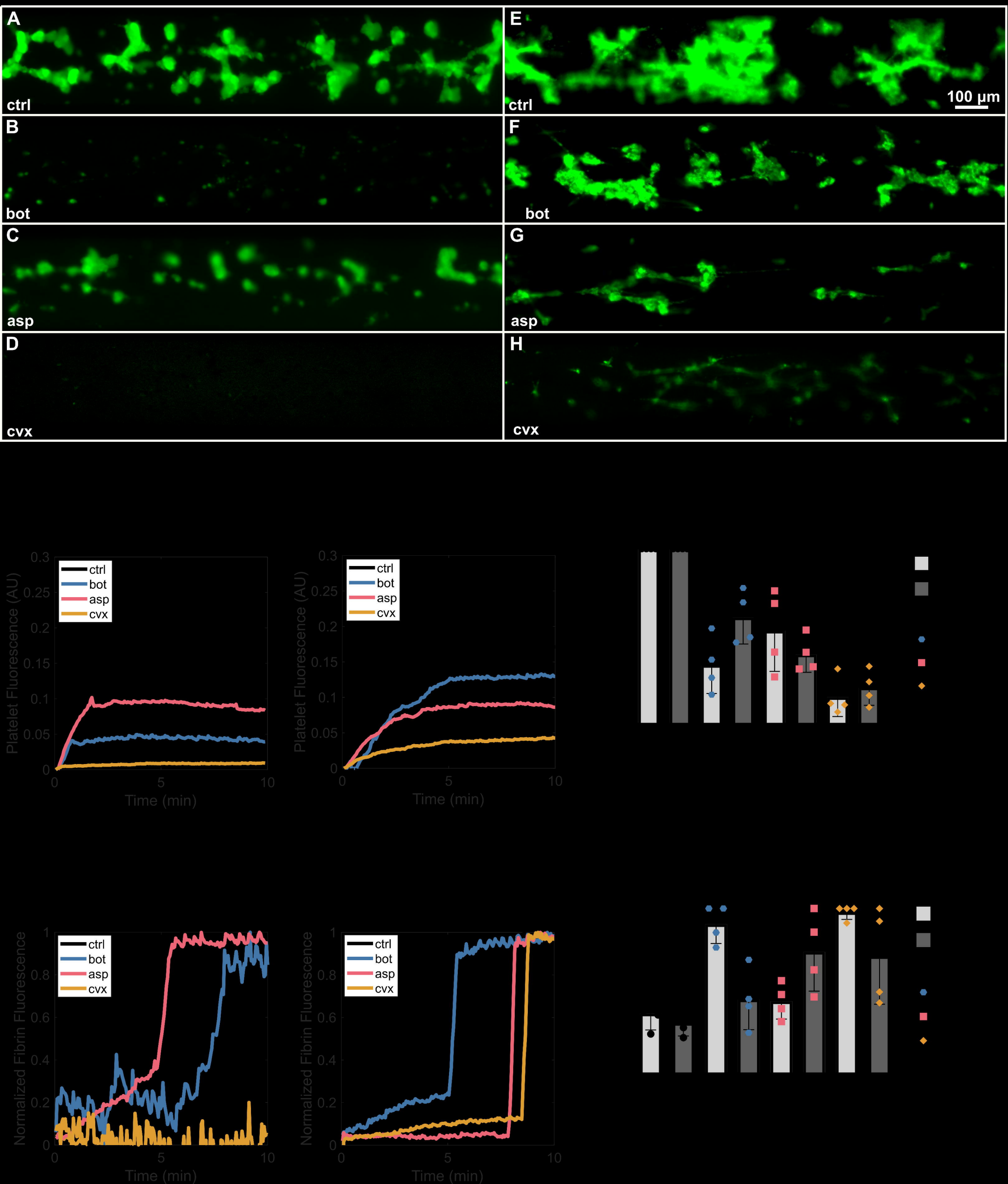
A
ctrl
B
bot
C
asp
D
cvx
E
ctrl
100 µm
F
bot
G
asp
H
cvx
ctrl
bot
asp
cvx
Platelet Fluorescence (AU)
Time (min)
Normalized Fibrin Fluorescence